PHYSICAL REVIEW B VOLUME 18, NUMBER 10 15 NOVEMBER, 1978

Theoretical studies of the optical and electronic properties of V, Nb, and Ta

J. F. Alward and C. Y. Fong
Department of Physics, University of California, Davis, California 95616

C. Guha Sridhar*
NASA-Ames Research Center, Moffett Field, California 94035

(Received 1 July 1977)

Band structures of V, Nb, and Ta have been calculated by the nonlocal empirical pseudopotential method (EPM). The bands have the same ordering and about the same shapes as previous first-principles results, but show important differences in the locations of the $N_{1'}$ and H_{12} states. It is shown that these differences suggest there is considerably less s-p and d-p hybridization of the augmented-plane-wave valence bands compared to the EPM bands. It is further shown that charge distributions with charge maxima located between *second* nearest neighbors occur when the H_{12} ($d_{x^2-y^2}$,d_{z^2}) states are more than 2.1 eV below the P_4 (d_{xy},d_{yz},d_{zx}) states. The present charge distributions provide a picture of partially metallic s-p bonding together with additional bonding associated with a "bilocal covalency" wherein a nearly nonoverlapping pair of tightly bound atomic d-like charge maxima are aligned between nearest-neighbor atoms. The theoretical reflectivity spectra, based on the direct-transition model (with $\vec{k}$-dependent matrix elements), are in reasonable agreement with the data by Weaver *et al*. The main structure in the optical reflectivity arises from transitions between hybridized s-d bands and hybridized s-p bands near the N symmetry point (e.g., $N_1 \rightarrow N_{1'}$). Reflectivities calculated with the nondirect-transition model are in unequivocally poorer agreement with the data than are the direct-transition reflectivities. The calculated densities of states and Fermi surfaces are shown to be in general agreement with available data. The partial densities of s, p, and d states are also presented.

I. INTRODUCTION

The group-V bcc transition metals, V, Nb, and Ta, have very high superconducting transition temperatures, and compounds containing these elements have the highest known transition temperatures.[1] Furthermore, these elements and their alloys have extremely high melting points. Because of the need to determine the origin of this unique combination of important physical properties, the results of a great many group-V electronic-energy-band structure calculations have been reported in the literature.[2-9,11-15,21-24] However, future use of these band structures as the basis of theoretical studies of these physical properties would be advisable only after it first has been determined that the band structures are consistent with all available experimental data. In this regard, comparisons to Fermi-surface and optical-reflectivity data deserve special attention since agreement with Fermi-surface data could establish the accuracy of the absolute locations of the bands *at* the Fermi level, and agreement with the optical-reflectivity data could help to verify the accuracy of the relative separations of the bands *near* the Fermi level. In the present study, surprising results are obtained which clearly illustrate that even agreement in *both* of these areas may not be sufficient to prove the accuracy of a given band structure because of the possibility that the band structure might still predict unrealistic charge distributions. In the remainder of this section the relatively large number of previous V, Nb, or Ta band-structure calculations will be briefly mentioned, and it will be especially noted which of these results explicitly demonstrates agreement with one or the other of the various types of experimental data.

Among the many early group-V transition-metal band-structure calculations are a modified-orthogonal-plane-wave (MOPW) band structure by Deegan and Twose,[2] a plane-wave Gaussian result for Nb by Euwema,[3] and augmented plane wave (APW) calculations for V by Mattheiss,[4] Snow and Waber,[5] Anderson *et al.*,[6] Hattox *et al.*,[7] and Bolemon.[8] None of these studies included calculations of Fermi surfaces, optical quantities, or charge densities, but nevertheless served usefully as the basis for later calculations.

In the literature there are many band-structure results which explicitly show agreement with Fermi-surface data, but none includes optical or charge-density studies. The first was by Mattheiss,[9] whose APW band structures for Nb and Ta are in good agreement with the Fermi-surface data by Halloran *et al.*[10] A later empirical pseudopotential method (EPM) calculation for Nb, by Fong and Cohen,[11] was fitted to Mattheiss' result and has since been seen by the authors to be in good agreement with Fermi surface data. Subse-

quent self-consistent (SC) APW calculations for Nb by Anderson *et al.*,[12] and for V by Papaconstantopoulos *et al.*,[13] and a tight-binding (TB)–OPW calculation for V by Yasui *et al.*,[14] are also in agreement with Fermi-surface data.

On the other hand, there are two studies which report the results of optical quantities—without Fermi-surface or charge densities. The first was by Pickett and Allen,[15] who used their Slater-Koster parametrization of Mattheiss's[9] Nb band structure to calculate the imaginary part ϵ_2 of the dielectric function—using the direct-transition model with constant dipole transition-matrix elements. The agreement with the data by Weaver *et al.*[16] is good but it is unclear how their calculated spectrum would be changed if the $\vec{k}$-dependent matrix elements were used. The second study was by Moruzzi *et al.*,[17] who obtained from their self-consistent APW bands of V a direct transition model conductivity spectrum which agrees to better than 0.5 eV with the data by Johnson and Christy.[18] However, neither the band structure nor a Fermi surface was reported, so one may not judge the accuracy of the bands at the Fermi level.

The results of optical calculations were also reported by Steel,[19] who used the densities of states results by Yasui *et al.*[14] and Papaconstantopoulos *et al.*[13] to obtain—from a nondirect transition model[20]—V absorptivity spectra which are in reasonable agreement with the data. However, it is not certain in his study whether the nondirect model is a good approximation to the more rigorous direct transition model which requires the use of $\vec{k}$-dependent dipole transition matrix elements. Indeed, it will be shown in Sec. III C that the present results obtained from the two models differ significantly.

Petroff and Viswanathan[21] determined an APW band structure for Ta and explicitly calculated the dipole matrix elements for use in a calculation of the energy distribution of photoemitted electrons. Unfortunately, Ta photoemission data is presently unavailable, so their results may not be used to evaluate the accuracy of the relative separations of their energy bands. No other optical quantity was obtained from their theoretical results.

The first explicit calculation of the charge distribution of one of the group-V transition metals was given for Nb by Ho *et al.*[22] Their result shows a stable distribution of charge, with absolute charge maxima located between nearest-neighbor atoms. No Fermi surface or optical quantity was calculated.

Finally, the present authors previously obtained EPM results for V,[23] and Ta,[24] which are in reasonable agreement with Fermi surface *and* reflectivity data. We have since discovered that these band structures and the one for Nb by Fong and Cohen[11] predict charge distributions in the (110) plane whose maxima occur between *second*-nearest-neighbor atoms, rather than between nearest neighbors. This is an unexpected result, especially in view of x-ray measurements on V which suggest charge maxima between nearest neighbors.[25] As will be noted in Sec. III B, these surprising results are caused by a specific inadequacy of the earlier EPM valence bands—an inadequacy which is eliminated in the present study.

In conclusion, several of the above studies provide agreement with Fermi surface data,[9,11-14,23,24] some show agreement with optical data,[13-15,23,24] and one provides a "correct" charge distribution,[22] but none explicitly demonstrates a charge distribution with nearest-neighbor maxima, *and* shows agreement with Fermi surface data *and* agreement with optical data. There is thus uncertainty about the accuracy of the bands either *at* the Fermi surface, or uncertainty regarding the *relative* locations of the bands *away* from the Fermi level, and an additional uncertainty arising from the possibility that the band structures might predict unusual charge distributions. The present work partially removes these uncertainties by using the empirical pseudopotential method to obtain V, Nb, and Ta band structures which predict stable charge distributions and which are also consistent with Fermi surface, photoemission, and reflectivity data.

In the Sec. II we give a brief discussion of the method of calculation, and in Sec. III we present the results of calculations of the band structures, charge densities, reflectivities, partial densities of states, and Fermi surfaces. A summary is given in Sec. IV.

II. METHOD

Since detailed discussions of the EPM have been given elsewhere,[24] we will mention here only the new feature of the present calculation.

As in the previous EPM calculations of Nb,[11] V,[23] and Ta,[24] about 135 plane waves are used and the potentials are characterized by a local and a nonlocal potential. The nonlocal potential is an attractive d well. Unlike these earlier calculations, we have found that the agreement with experiment is improved by the additional use of a nonlocal, attractive p well. The need for an attractive nonlocal p well was also reported by Ho *et al.*[22] in an independent study of Nb. The present need for an attractive p well is in contrast to the situation found by Fong and Cohen[26] for the noble metals. In gold and silver, the p-like conduction states experience substantial screening of the nucleus by

the completely filled d states (e.g., Cu[Ar] $3d^{10}4s^1$) which form a nearly spherical distribution of charge about the atom. In these crystals, then, a lowering of the p-like states via an attractive p well is not necessary. However, in the Group V transition metals the d states are incompletely filled (e.g., Nb[Kr] $4d^45s^1$) so the unoccupied p states would be expected to be lower in energy because of a stronger attraction by the nucleus. As will be noted in Sec. III, the presence of the p wells is the source of the most important differences between the present results and the APW results.

III. RESULTS

A. Energy-band structures

Energy-band structures for V, Nb, and Ta are shown in Fig. 1. The horizontal lines indicate the zero of energy, taken at the respective Fermi levels E_F. The EPM parameters corresponding to these band structures are listed in Table I. The important energy gaps for these and the various earlier band structures are shown in Table II. We will first discuss differences among the present band structures, and then contrast these results with the various APW calculations.

1. Comparison of present band structures

The present band structures have the same band ordering, and corresponding bands have essentially the same shapes. The most noticeable difference among the band structures is in the location of the s-like Γ_1 states. With respect to E_F, Γ_1 in V is at −6.06 eV, −4.58 eV in Nb, and −3.78 eV in Ta. The s states are thus more tightly bound in V, less so in Nb, and least tightly bound in Ta. The lo-

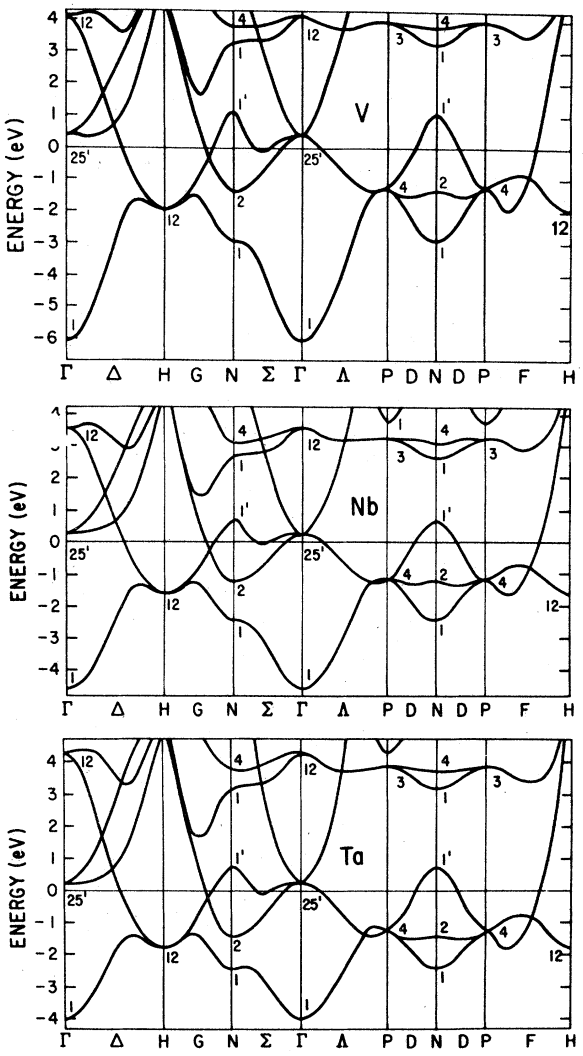

FIG. 1. EPM band structures of V, Nb, and Ta.

TABLE I. Comparison between the present and previous EPM parameters for V, Nb, and Ta.

	$v(2)$[a] (Ry)	$v(4)$ (Ry)	$v(6)$ (Ry)	$v(8)$ (Ry)	V_p (Ry)	R_p (Å)	V_d (Ry)	R_d (Å)	α	κ $(2\pi/a)$	γ $(10^{-49}$ g cm$^3)$	a (Å)
					Present results							
V	−0.035	0.060	−0.034	0.110	−0.820	0.970	−6.600	0.918	0.219	1.668	1.260	3.025
Nb	−0.047	0.107	0.012	0.130	−0.630	1.104	−4.653	1.044	0.206	1.668	0.590	3.300
Ta	−0.055	0.094	0.005	0.130	−0.450	1.200	−3.783	1.136	0.206	1.668	0.590	3.300
					Previous results							
V[b]	−0.052	−0.002	−0.008	0.084	•••	•••	−6.100	1.000	0.220	1.668	0.800	3.025
Nb[c]	−0.041	−0.020	−0.009	0.070	•••	•••	−3.884	1.136	0.206	1.668	•••	3.300
Ta[d]	−0.041	0.100	0.071	0.150	•••	•••	−3.483	1.136	0.206	1.668	1.100	3.300

[a] The arguments of the form factors $v(|\vec{G}|^2)$ are in units of $(2\pi/a)^2$, where a is the lattice constant.
[b] Reference 23.
[c] Reference 11.
[d] Reference 24.

TABLE II. Comparison of important energy gaps in the group-V transition-metal band structures.

V	E_F-Γ_1	$\Gamma_{25'}$-E_F	E_F-H_{12}	$N_{1'}$-E_F	$N_{1'}$-N_1	E_F-P_4	P_4-H_{12}
Mattheiss[a] (APW)	6.94	0.31	3.29	...	...	...	...
Anderson *et al.*[b] (APW, $\alpha=1$)	5.67	0.84	2.90	1.32	4.11	...	...
Yasui *et al.*[c] (SC, MOPW, $\alpha=0.725$)	5.98	0.19	2.15	2.09	5.07	1.08	1.07
Papaconstantopoulos *et al.*[d] (SC, APW, $\alpha=\frac{2}{3}$)	6.76	0.63	3.28	1.17	4.60	1.18	2.20
Hattox *et al.*[e] (SC, APW, $\alpha=0.715$)	6.29	0.38	2.99	1.69	4.72	...	...
Alward *et al.*[f] (EPM)	6.53	0.56	4.06	2.29	6.02	0.96	3.09
Present results	6.60	0.37	1.96	1.06	4.00	1.33	0.59
Nb							
Mattheiss[g] (APW)	5.34	0.38	3.92	2.33	5.94	1.06	2.85
Fong and Cohen[h] (EPM)	5.25	0.46	3.53	2.13	5.39	0.94	2.59
Anderson *et al.*[i] (SC, APW, $\alpha=\frac{2}{3}$)	5.26	0.56	4.24	2.26	6.00	1.02	3.22
Pickett and Allen[j] (Slater-Koster)	5.41	0.29	4.18	2.27	5.85	1.01	3.29
Ho *et al.*[k] (SC pseudopotential)	6.06	0.15	3.22	2.32	5.81	1.18	2.04
Present results	4.58	0.29	1.61	0.69	3.09	1.13	0.48
Ta							
Mattheiss[g] (RAPW)	7.63	0.35	3.87	1.44	5.76	1.20	2.81
Petroff and Viswanathan[l] (APW)	5.49	0.53	4.11	2.57	6.31	1.01	3.10
Alward *et al.*[m] (EPM)	5.50	0.45	3.37	1.92	5.15	0.81	2.56
Present results	3.98	0.21	1.79	0.74	3.15	1.24	0.55

[a]Reference 4.
[b]Reference 6.
[c]Reference 14.
[d]Reference 13.
[e]Reference 7.
[f]Reference 23.
[g]Reference 9.
[h]Reference 11.
[i]Reference 12.
[j]Reference 15.
[k]Reference 22.
[l]Reference 21.
[m]Reference 24.

cation of the Γ_1 state in V is in fair agreement with the soft x-ray data by Fischer[27] (−6.4 eV), and its location in Nb is in agreement with the experimental results obtained by Holliday,[28] and by Nemoshkalenko and Krivitskii[29] (~5 eV). The authors have not found similar Ta data in the literature.

Another point of difference among the present band structures is in the separation between the N_1 (sd) and N_1' (p) states, located below and above the Fermi level, respectively. As noted in Table II, the N_1'-N_1 separation is largest in V. The separation is greatest in V primarily because of the smaller lattice constant (3.025 Å, vs 3.300 Å for Nb and Ta) which forces a comparatively larger overlap between p states of neighboring atoms. The larger overlap thus forces the p-like states to higher energies. The relative elevation of the V p-like states is consistent with the observations by Kmetko,[30] who calculated the radial charge densities for reduced lattice spacings in various metals and found that the effect of compression in simple metals is to raise the p-like states.

2. Comparison of present (EPM) and past (APW and EPM) bands

Within about 5 eV of the Fermi level, the present EPM bands for V, Nb, and Ta have the same ordering and roughly the same shapes as the earlier APW and EPM bands. The two most important quantitative differences are discussed below (see also Table II).

The present locations of the N_1' states are about an average of 1.15 eV lower than the N_1' states in the earlier calculations; this result suggests the present bands have comparatively larger s-p and d-p hybridization compared to the APW results. This difference may in part be due to the absence of any p-like character in the charge configuration used to obtain the first-principles potentials, while the present EPM potentials were explicitly chosen to have an attractive influence on the p-like states. The important influence of the location of N_1' on the calculated optical properties will be discussed in Sec. III C.

Another significant difference between the present and previous band-structure calculations is in the relative location of the H_{12} and P_4 states. In the present study, the P_4-H_{12} separation is an average of 2.07 eV smaller compared to previous EPM[11,23,24] and first-principles[2-9,12-15,21] calculations. This rather large difference can be understood on the basis of increased d-p and s-p hybridization. If additional p-like states are to be pulled below the Fermi level, then it must be done primarily at the expense of the d states which

comprise the majority of the valence states. Since the P_4 states (d_{xy}, d_{yz}, d_{zx}) are triply degenerate, they naturally make the greatest contribution to the occupied density of states. Thus, the placement of the Fermi level should be quite sensitive to changes in the location of P_4, and less sensitive to the location of other states. Indeed, Table II shows that the mean deviation from the average value of E_F-P_4 for 14 earlier band structure calculations is quite small (about 0.1 eV), while the mean deviation for the E_F-H_{12} separation is relatively large (0.68 eV). Thus, increasing the d-p hybridization will force the d states upward, with the doubly-degenerate H_{12} states moving farther than the triply degenerate P_4 states, which are tightly pinned to the Fermi level. The critical relationship between the value of the P_4-H_{12} separation and the location of the maxima in the charge densities will be discussed in considerable detail in the following section.

B. Charge distributions in the (110) plane

As noted above, improvements over earlier EPM results[11,23,24] became necessary when the authors recently used these earlier band structures to calculate charge densities and found that the maxima of charge appeared between *second*-nearest neighbors instead of between *nearest* neighbors. The charge distribution based on the earlier Nb EPM band structure is shown in Fig. 2. In this figure is shown the cross section of the total valence band charge density in the diagonal (110) plane of the bcc unit cell. Note the locations of the maxima are between *second*-nearest neighbors. This configuration is unstable because any disturbance which would lead to a movement of these maxima toward a nearest-ion location would cause a permanent dislocation of the maxima.

We have traced the origin of these unusual results to a specific inadequacy of the associated band structures. We found that whenever the doubly degenerate H_{12} states are more than about 2.1 eV below the triply degenerate P_4 states, the corresponding total valence band charge densities display maxima between *second*-nearest neighbors. The dependence of the maxima location on the separation between these states may be understood with the help of Figs. 3 and 4. Figure 3 shows the result of a calculation of the diagonal-plane charge density associated with the H_{12} states alone. The symmetry type of these states are indicated in the figure—a state of $d_{x^2-y^2}$ symmetry, and a state of d_{z^2} symmetry. Since the diagonal plane is a nodal surface for the $d_{x^2-y^2}$ states, these states contribute no charge in the diagonal plane. However, the effect of the d_{z^2} states is obvious: The plus lobes give rise to the large concentration of charge located above and below the body-centered atom, while the minus ring corresponds to the smaller lobes to the right and left of this atom. For the triply degenerate P_4 states, whose charge

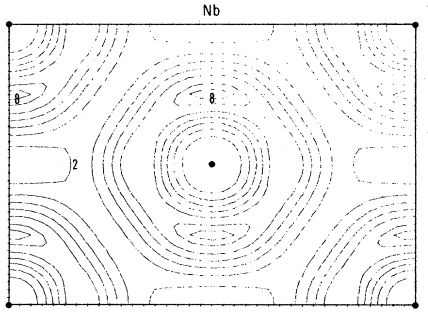

FIG. 2. Charge density in the (110) plane, based on the Nb EPM band structure by Fong and Cohen (Ref. 11). Charge maxima are located between second-nearest neighbors.

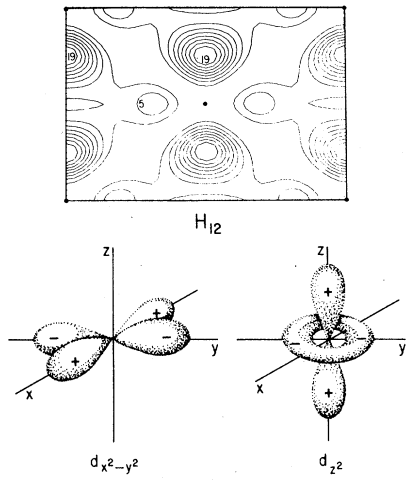

FIG. 3. (110) charge distribution for the H_{12} states.

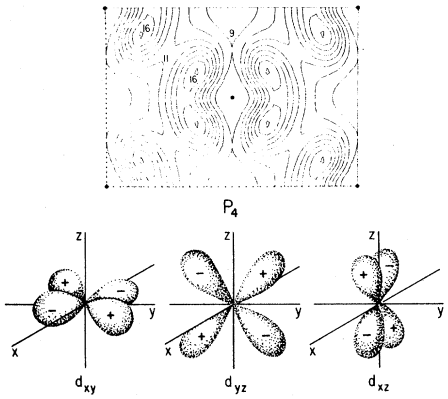

FIG. 4. (110) charge distribution for the P_4 states.

distribution is shown in Fig. 4, a linear combination of the three states causes maxima to appear between the nearest neighbors. The numbers appearing within the H_{12} and P_4 charge distributions correspond to the relative strengths and suggest the close competition for dominance which can occur between the $d_{x^2-y^2,z^2}$ and $d_{xy,yz,zx}$ states in the *total* valence band charge distributions. If P_4 is too high relative to H_{12}, then the $d_{x^2-y^2,z^2}$ states will be dominant valence band states, thereby masking the effects of the $d_{xy,yz,zx}$ states and producing maxima between second-nearest neighbors. This masking is evident in the charge distribution which we based on the earlier Nb band structure (Fig. 2). The value of the P_4-H_{12} separation in the earlier[11] Nb EPM band structure is 2.58 eV and is considerably larger than that obtained in the present Nb band structure (0.48 eV). There is a similarly striking contrast between the previous[24] and the present Ta calculations (2.56 vs 0.55 eV). As noted in Table II, earlier band structure calculations for V, Nb, and Ta predict values of the P_4-H_{12} separation which are more than 1.5 eV larger than the present results. One of the smallest previous values is found in the pseudopotential result by Ho *et al.*[22] In that calculation it is probably not merely coincidental that their charge distribution, which is the first to be explicitly calculated for one of the group-V transition metals, is obtained from a band structure with a P_4-H_{12} separation less than the critical value of 2.1 eV found in the present study. Of the eighteen existing group-V band-structure calculations, the only other result which shows a P_4-H_{12} gap below 2.1 eV is that by Yasui *et al.*[14]

The results of the present calculations of the total valence charge distributions in the (110) planes of V, Nb, and Ta are shown in Fig. 5. There are atoms at the center and four corners of the figures. Since the present pseudo-wave-functions are not orthogonalized to the core states, the distribution of charge very near the atoms may not be representative of the true charge density. However, this possible inaccuracy does not vitiate our results for those charges which play the dominant role in determining the electronic and optical properties of these elements—the interstitial charges. An arbitrary numbering scheme provides the relative strengths of the contours.

The total valence charge densities for the three elements are very similar, each having a strong atomiclike character wherein the charge about each atom resembles that which would be expected about isolated atoms. The nearly spherical contours very close to and surrounding each atom correspond to the *s*-like states, while the banana-shaped lobes on either side of each atom are

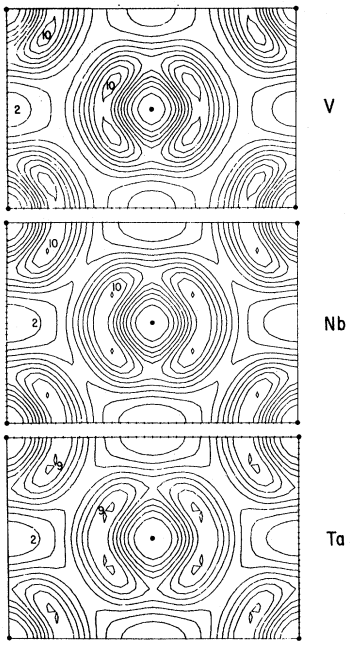

FIG. 5. Present charge densities for V, Nb, and Ta. Charge maxima are located between nearest neighbors.

hybridized *pd* states. Four small, is landlike maxima about each atom are located about $\frac{1}{4}$ of the distance between nearest atoms and are formed from a superposition of the d_{xy}, d_{xz}, and d_{yz} states. In Ta, these "islands" each appear as two barely separated smaller islands. There is no physical significance for this separation; the separation is an artifact caused by the relative coarseness of the grid in which the charge density was calculated (37×37).

Elsewhere within the interstitial region the distribution is roughly uniform and arises primarily from the *s*- and *p*-like states. The overall picture which emerges is that of *d*-like charge firmly attached to nuclei, which themselves are imbedded within a sea of comparatively uniform *s*-*p* charge.

The pairs of island maxima which appear between nearest-neighbor atoms (doublet pairs for Ta) provide a joint screening of the their corresponding nuclei. The tightly bound nature of the *d* states prevent the formation of a single cluster of overlapping charge and instead produces a pair of clusters which provide bifold screening of the nearest-neighbor nuclei. Truly covalent bonding, in which the covalent bond is associated with a *single* cluster of overlapping charge, is thus not seen in the present results, so the bonding here might be more correctly described as being partially metallic, due to the interstitial *s*-*p* charges, and partially "bilocally covalent."

The present discussion of the *d*-*p* hybridization

in the pure transition metals is particularly relevant to the recent study by Miedema[31] of several hundred binary alloys. Miedema noted that d-p hybridization makes a large negative contribution to the heat of formation of alloys of transition metals with nontransition metals. This contribution is characterized by the R term in Eq. (4) of Ref. 31. While it is at present difficult to make a quantitative estimate of the extent of d-p hybridization which would arise if the interaction were between pure d-like states of the transition metal and pure p-like states of the nontransition metal, one would nevertheless expect that the hybridized d-p states of the transition metals would interact even more strongly with the p-states of the nontransition metal. The present results thus suggest the hybridized d-p states of the transition metal would be an important consideration in any future search for the microscopic origins of the R term in Miedema's scheme.

C. Reflectivities

The results of calculations of the reflectivities of V, Nb, and Ta are compared in Figs. 6–8 to the data by Weaver *et al.*[16,32] For each element, the theoretical calculations predict spectral shapes below 5 eV which are in general agreement with the shapes of the experimental curves. The agreement of the locations of the main structure suggests that the relative positions of the energy bands within about 2–3 eV of the Fermi level are accurate to about 0.5 eV, because the locations of the main structure below 4 eV in each element agree to within about 0.5 eV with the data. In several preliminary calculations the authors found that the pseudopotential form factors could be adjusted by amounts not greater than 0.02 Ry to obtain reflectivity spectra with improved agreement with the data—to within 0.2 eV. However, such

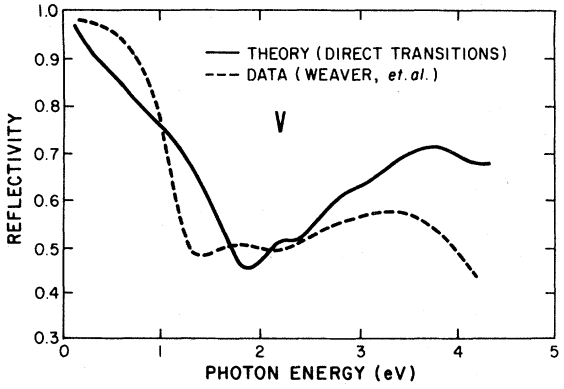

FIG. 6. Theoretical reflectivity spectrum of V, compared to the data by Weaver *et al.* (Ref. 32).

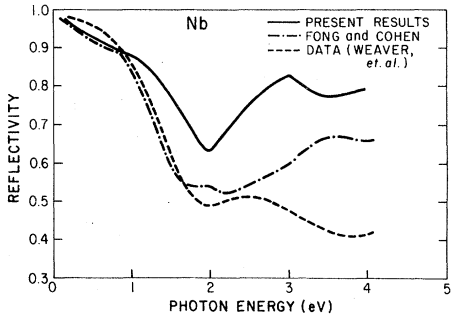

FIG. 7. Theoretical reflectivity spectrum of Nb, compared to the theoretical result by Fong and Cohen (Ref. 11) and the data by Weaver *et al.* (Ref. 16).

adjustments always led to a worsening of the agreement with Fermi-surface data (Sec. III E). The present reflectivity results thus represent the best possible compromise with the Fermi-surface data.

The majority of the strength (~60%) below 4 eV in the reflectivity spectra is due to transitions between first and third bands (1-3 transitions) near the N symmetry point. While the strongest of the 1-3 transitions occur at the N symmetry point ($N_1 \rightarrow N_{1'}$), the majority of the strength near N comes from a region near the off-symmetry point, $\vec{k}=(\frac{1}{2},\frac{1}{2},\frac{1}{6})2\pi/a$.

Due to the unavailability at that time of optical data, the first EPM Nb band structure was fit by Fong and Cohen[11] to the APW results by Mattheiss.[9] It has since been noted that both of these results are in good agreement with photoemission data.[33] However, we have already noted that the former EPM Nb result predicts an unstable charge distribution. Furthermore, as shown in Fig. 7, the main strength below 4 eV in the earlier Nb spectrum is more than 1 eV higher than the main peak in the data, while the present spectrum agrees with the data to within about 0.5 eV. These results serve to illustrate the danger involved in

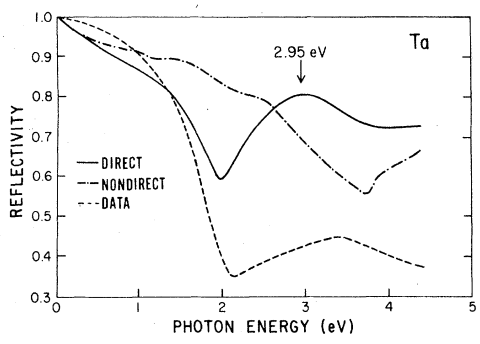

FIG. 8. Ta reflectivity spectra, based on the direct (solid curve) and nondirect (chain curve) transition models, are compared to the data (broken curve) by Weaver *et al.* (Ref. 32).

an exclusive reliance upon a single criterion—such as agreement with photoemission data along—to judge the accuracy of an EPM band structure. Indeed, as the authors have found in the previous studies of V,[23] and Ta,[24] even reasonable agreement with photoemission, reflectivity, and Fermi-surface data is not sufficient to guarantee the accuracy of EPM band structures.

Finally, while the previous Ta band structure[24] predicts a theoretical reflectivity spectrum which is roughly independent of whether the direct or the nondirect transition model is used, the present results unequivocally favor the direct transition model. To the authors' knowledge, these results are the first in which it is explicitly demonstrated that the direct transition model is conclusively superior to the nondirect model in theoretical studies of the optical spectra of transition metal elements. A comparison in Fig. 8 of calculations of the Ta reflectivity, based on each model, shows that the nondirect transition model predicts a virtually structureless reflectivity spectrum, while the direct transition model is in reasonable agreement with the data and shows several prominent structures. The direct and nondirect spectra compare to one another just as unfavorably in V and Nb as in Ta. (The nondirect spectra for V and Nb are not shown.) The striking contrast between the present and the past[24] comparisons of direct and nondirect models is caused primarily by the relative lowering of the N_1' states in the present calculations. In the previous EPM results[11,23-24] the separation between N_1 and N_1' is too large to significantly influence the calculated optical properties below 4 eV. The optical strength in those results is due to a large number of weak d-d transitions from all over the zone (volume transitions). In the present work, however, the N_1-N_1' (sd-p) separations are within the range of interest (below 4 eV) and the large dipole transition matrix elements associated with transitions between these states play an important role in the direct transition calculation of the optical reflectivity. The arrow at 2.95 eV in the present direct transition Ta reflectivity spectrum indicates the location of the main peak. This location correlates well with the N_1-N_1' separation of 3.15 eV (see Table II). We have already noted that the APW p states are high compared to the present EPM results. Just as in the earlier EPM results[11,23,24] the p states would not be expected to have much influence on the calculated optical properties of these elements. The main APW optical transitions would be between d-like states, so any variations in the matrix elements would not be large. One might expect, then, that APW results of direct transition optical calculations would be similar to the results of nondirect, constant matrix elements calculations.

D. Densities of states

The partial densities of s-, p-, and d-like states, and the total densities of states (DOS) are shown in Figs. 9(a) and 9(b) for V and Ta. The results for Nb are not shown because the main features of the Nb DOS are similar to those for Ta. The qualitative features of the densities of states are similar. For each element, roughly 50% of the states below the Fermi level are d like, 25% s like, and 25% p like.

The present total densities of states for V and Nb are in general agreement (to within 0.2 eV) with the optical densities of states (ODS) obtained from photoemission spectroscopy (PES) measurements by Eastman,[33] using a nondirect transition model (again, only the V results are shown; the agreement of the Nb results is comparable to that for V). Similar data for Ta are not available.

Since it is somewhat uncertain to what extent nondirect transition occur during multiscattering photoemission processes, the present agree-

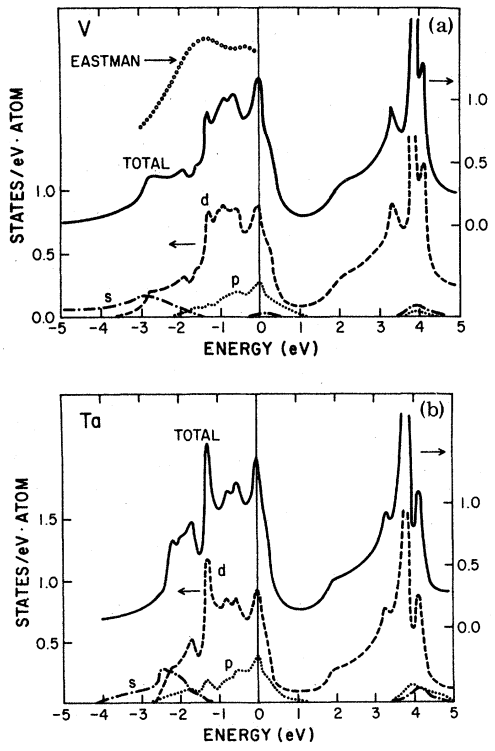

FIG. 9. (a) Partial densities of states of V. The total density of states is compared to the optical density of states obtained by Eastman (Ref. 33). (b) Partial densities of states of Ta. No photoemission data are available for comparison.

ments—and disagreements—of the DOS with Eastman's ODS should not serve as an important indication of the overall accuracy of the present band structures. Indeed, the previous EPM Nb calculation[11] predicts a DOS whose main peaks correlate well (~0.2 eV) with the peaks in the photoemission data, even though that band structure predicts an unstable charge distribution (Sec. III B) and a reflectivity spectrum (Sec. III C), which is in poor agreement with experiment.

E. Fermi surfaces

Fermi-surface cross sections for V, Nb, and Ta are shown in Fig. 10. Theoretical contours are indicated by the solid curves, and experimental contours, for V by Parker and Halloran[34] and for Nb and Ta by Halloran *et al.*,[10] are shown as broken curves. It has been assumed for convenience that the measurements correspond to perfect ellipsoids, and the ellipsoidal dimensions have been determined accordingly.

Hole pockets of approximate ellipsoidal shape are predicted about the N symmetry point for each element. To test the sensitivity of the Fermi surface shape to the location of the Fermi level, the authors varied the location of the Fermi level artificially, in amounts of ±0.2 eV and found that the calculated areas of the ellipsoidal cross sections changed by ∓20%. Since the present agreements are to within 15%, these results suggest that the absolute locations of the bands at the Fermi level are accurate to better than 0.2 eV. It would have been possible to adjust the potentials so that agreement with Fermi surface data would be better than 3%, but it was found that such an adjustment leads to a worsening of agreement with reflectivity data. The present agreements represent the best possible compromise.

Hole surfaces about the Γ symmetry point are predicted here for V, Nb, and Ta. However, Halloran *et al.*[10] and Parker and Halloran[34] were unable to make unambiguous measurements of these hole pockets, probably—as noted by Parker and Halloran—because of the low signal strength caused by the high effective electron mass near this surface. Nevertheless, hole pockets about Γ have been predicted in several earlier calculations.[9,11-14,23,24]

The so-called jungle-gym arms are prominent features of the theoretical Fermi surfaces and have also been observed experimentally.[10,34] Halloran *et al.*[10] indicate that "necks" joining the ellipsoids to the jungle-gym are absent in Nb and Ta, but the measurements by Parker and Halloran[34] support their existence in V. However, the present results can not categorically confirm or deny

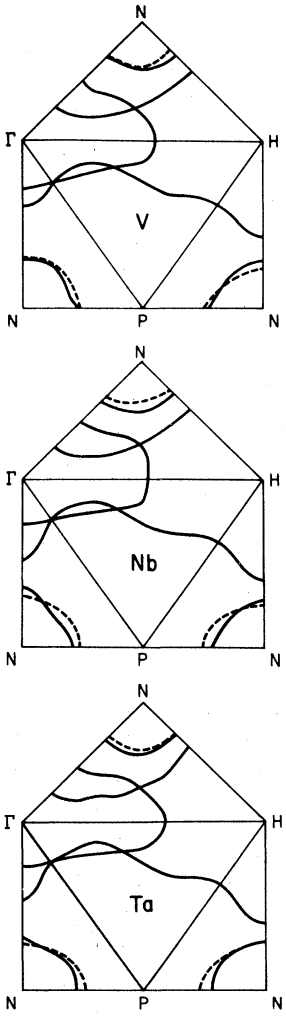

FIG. 10. Theoretical (solid curves) and experimental (broken curves) Fermi surfaces for V, Nb, and Ta.

the existence of these necks. Regarding the origin of these necks, we should note that if the Σ_1 band did not dip below the Fermi level, the ellipsoids would then open along the ΓN direction and form necks leading into the jungle gym. Since the absolute locations of the present energy bands near the Fermi surface are known only to within about 0.2 eV, while the Σ_1 band dips only 0.1–0.2 eV below E_F, the present results thus suggest the possibility that very narrow necks exist in the Fermi surface of pure laboratory specimens. We estimate they would probably have extremal diameters no larger than about $\frac{1}{25}\,2\pi/a$.

IV. SUMMARY

The empirical pseudopotential method has been used to obtain energy band structures for V, Nb, and Ta, and from these band structures we have calculated the charge distributions, reflectivities, partial densities of states, and Fermi surfaces.

It is perhaps easiest to simply list our findings below.

(i) The V, Nb, and Ta EPM band structures are similar in shape and band ordering, the largest difference being in the locations of the Γ_1 state, which in V is roughly 2 eV lower than in Nb or Ta. This comparison suggests that the s-like states of V are more tightly bound than in Nb or Ta.

(ii) Two main differences between the present band structures and the earlier APW band structures are in the locations of the p-like N_1' state, which are closer to the Fermi level in our band structures, and in the values of the P_4-H_{12} energy gaps, which are an average of 2.62 eV in the APW results, but average only 0.55 eV in the present results. Each of these important differences arise because the present potentials have greater p-like character than the earlier EPM and APW potentials.

(iii) Because of the competition between states of d_{z^2} and d_{xy}-type symmetry, the maxima of the charge distribution in the (110) plane switches from a nearest-neighbor to a second-nearest-neighbor location whenever the H_{12} $(x^2 - y^2, z^2)$ states drop more than about 2.1 eV below the P_4 (xy, yz, zx) states.

(iv) Maxima of the charge distributions in the (110) plane of all three elements arise from a linear superposition of d_{xy}, d_{yz}, and d_{zx} states; these maxima are located $\frac{1}{4}$ of the distance between nearest-neighbor atoms.

(v) Bonding in V, Nb, and Ta is partially metallic, with additional bonding provided by a "bilocal covalent" bond, wherein charge maxima from tightly bound, atomic-like d states align—but do not significantly overlap—between nearest-neighbor atoms.

(vi) Below $\hbar\omega = 4$ eV transitions from bands connecting N_1 to bands connecting N_1' provide the largest contribution to the calculated strength in the reflectivity spectra.

(vii) The direct transition reflectivity spectra for V, Nb, and Ta agree with the data below 4 eV to within 0.5 eV, indicating that the relative separations of the energy bands are accurate to within 0.5 eV.

(viii) The direct transition model has been shown to be in unequivocally better agreement with the data than is the nondirect model.

(ix) The theoretical Fermi surfaces agree to within 15% with the Fermi surface data, indicating that the bands at the Fermi level are accurate to better than 0.2 eV. The present results cannot categorically rule out the possibility that the hole ellipsoids about N are connected by narrow "necks" to the jungle gym.

It has been emphasized in this work that exclusive reliance upon a Fermi surface to judge the accuracy of a given band structure is inadvisable, and that even the additional use of theoretical Fermi surfaces and reflectivities may be inadequate for such evaluations because of the sensitive dependence of charge maxima location on the location of H_{12}.

ACKNOWLEDGMENTS

The authors gratefully acknowledge comments and suggestions by J. C. Phillips, P. B. Allen, J. H. Weaver, and S. G. Louie. Two of us (J. F. A. and C. Y. F.) were supported in part by the U. S. AFOSR (AFSC) under Contract No. F49620-76-C-0016. Funds for part of this study by one of us (C. G. S.) have been provided by NASA-Ames Research Center, Moffett Field, Calif. under interchange NCA2-OR180-502.

*Present address: 28-C Beacon Village Apts., Burlington, Mass. 01803.

[1]B. W. Roberts, *Progress in Cryogenics* (Heywood, London, 1964); F. Heininger, E. Bucher, and J. Muller, Phys. Kondens. Mater. 5, 243 (1966).
[2]R. A. Deegan and W. D. Twose, Phys. Rev. 164, 993 (1967).
[3]R. N. Euwema, Phys. Rev. B 4, 4332 (1971).
[4]L. F. Mattheiss, Phys. Rev. 134, A1970 (1964).
[5]E. C. Snow and J. T. Waber, Acta Metall. 71, 623 (1969).
[6]J. R. Anderson, J. W. McCaffrey, and D. A. Papaconstantopoulos, Solid State Commun. 7, 1439 (1969).
[7]T. M. Hattox, J. B. Conklin, Jr., J. C. Slater, and S. B. Trickey, J. Phys. Chem. Solids 34, 1627 (1972).
[8]J. S. Bolemon and C. P. Poole, Bull. Am. Phys. Soc. 14, 612 (1969).
[9]L. F. Mattheiss, Phys. Rev. B 1, 373 (1970).
[10]M. H. Halloran, J. H. Condon, J. E. Graebner, J. E. Kunzler, and F. S. L. Hsu, Phys. Rev. B 1, 366 (1970).
[11]C. Y. Fong and M. L. Cohen, Phys. Lett. A 44, 375 (1973).
[12]J. R. Anderson, D. A. Papaconstantopoulos, J. W. McCaffrey, and J. E. Schirber, Phys. Rev. B 7, 5115 (1973).
[13]D. A. Papaconstantopoulos, J. R. Anderson, and J. W. McCaffrey, Phys. Rev. B 5, 1214 (1972).
[14]M. Yasui, E. Hayashi, and M. J. Shimizu, Phys. Soc. Jpn. 29, 1446 (1970).
[15]W. E. Pickett and P. B. Allen, Phys. Rev. B 11, 3599 (1975).
[16]J. H. Weaver, D. W. Lynch, and C. G. Olson, Phys. Rev. B 10, 4311 (1973).
[17]V. L. Moruzzi, A. R. Williams, and J. F. Janak (private communication to P. B. Johnson and R. W. Christy, Ref. 18).
[18]P. B. Johnson and R. W. Christy, Phys. Rev. B 9,

5056 (1974).
[19]M. R. Steel, J. Phys. F 4, 783 (1974).
[20]The nondirect model assumes that all transition occur with equal probability and that the rate of transitions of a given photon energy $\hbar\omega$ is proportional to the quantity $\omega^{-2}\Sigma_E n(E+\hbar\omega)n(E)$, where the summation is over valence and conduction bands, $E+\hbar\omega$ is the conduction-band energy, E is the valence-band energy, and n is the total density of states.
[21]I. Petroff and C. R. Viswanathan, Phys. Rev. B 4, 799 (1971).
[22]K. M. Ho, S. G. Louie, J. R. Chelikowsky, and M. L. Cohen (private communication).
[23]J. F. Alward, C. M. Perlov, C. Y. Fong, and C. Guha Sridhar, Bull. Am. Phys. Soc. 21, 245 (1976).
[24]J. F. Alward, C. Guha Sridhar, C. M. Perlov, and C. Y. Fong, Phys. Rev. B 15, 5724 (1977).
[25]R. J. Weiss and J. J. Demarco, Phys. Rev. 140, A1223 (1965); M. Fujimoto, O. Terasaki, and D. Watanabe, Phys. Lett. A 41, 159 (1972); M. V. Linkoaho, Phys. Scr. 5, 271 (1972).
[26]C. Y. Fong and M. L. Cohen, Phys. Rev. Lett. 24, 306 (1970).
[27]D. W. J. Fischer, J. Appl. Phys. 40, 4151 (1969).
[28]J. E. Holliday, in *The Electron Microscope*, edited by T. D. McKinley, K. F. J. Meinrich, and D. B. Wittry (Wiley, New York, 1966), p. 10.
[29]V. V. Nemoshkolenko and V. P. Krivitskii, Ukr. Fiz. Zh. 13, 1274 (1968) [Ukr. Phys. J. 13, 911 (1969)].
[30]E. A. Kmetko, Phys. Rev. A 1, 37 (1970).
[31]A. R. Miedema, J. Less-Common Metals, 41, 283 (1975).
[32]J. H. Weaver, D. W. Lynch, and C. G. Olson, Phys. Rev. B 10, 501 (1974).
[33]D. E. Eastman, Solid State Commun. 7, 1679 (1969).
[34]R. D. Parker and M. H. Halloran, Phys. Rev. B 9, 4130 (1974).